Plastic Semiconductor Solid Solutions Ag₂S–Ag₂Se

**Yu. S. Tveryanovich[a], *, E. V. Smirnov[a], A. S. Tveryanovich[a], V. V. Tomaev[a, c], O. V. Glumov[a],
O. V. Tolochko[b], I. A. Kasatkin[a], and A. A. Abramovich[a]**

[a] *Institute of Chemistry, St. Petersburg State University, St. Petersburg, 198504 Russia*
[b] *St. Petersburg Polytechnic University, St. Petersburg, 195251 Russia*
[c] *St. Petersburg Institute of Technology, St. Petersburg, 190013 Russia*
*e-mail: y.tveryanovich@spbu.ru

Abstract—Semiconductor solid solutions in the Ag₂S–Ag₂Se system are studied. It is shown that monoclinic solid solutions based on Ag₂S have a plasticity exceeding that of silver sulfide and selenide. The possibility of obtaining wire and foil from them by cold rolling is demonstrated. The concentration dependencies of the optical band gap and the Seebeck coefficient are studied. It is shown that intensive deformation (cold rolling) does not lead to a change in the parameters of the temperature dependencies of the electrical conductivity.

INTRODUCTION

The intensive development of flexible electronics requires the creation of new semiconductor materials. Semiconductor materials currently used in flexible electronics can be divided into three main groups: inorganic nanocrystalline (including carbon), inorganic amorphous, and organic semiconductors. The first group of materials has relatively stable functional properties, but low flexibility and plasticity. Organic semiconductors are quite plastic, but their properties degrade relatively quickly. Amorphous semiconductors, represented mainly by amorphous silicon, occupy an intermediate position in this series and have difficult-to-control electronic properties. Therefore, the discovery of plasticity characteristic of metals in crystalline semiconductors Ag₂S [1] and Ag₂Se [2, 3] opens a new direction in the development of semiconductor materials for flexible electronics. The importance of this direction is also determined by the fact that the entire existing electronics industry is adapted to work with crystalline inorganic semiconductors and changing this direction is associated with enormous problems.

The existence of plastic inorganic crystalline semiconductor materials is paradoxical. Indeed, semiconductor properties are provided by covalent interatomic interactions. Covalent bonds are known to be directional and short-range. Therefore, the substances they form must be fragile. In [2, 3] this paradox is explained by the coexistence of two subsystems of interatomic bonds in crystals: covalent metal-chalcogen bonds and metallophilic metal-metal bonds. Each of these subsystems forms a three-dimensional continuous grid. The importance of the nature of chemical interaction for the emergence of plasticity of semiconductor substances is confirmed by the fact that the introduction of Ag₂Se in the composition of chalcogenide glasses also leads to a significant increase in their plasticity [4].

Interest in the Ag₂S–Ag₂Se system is due to a variety of reasons. The presence of solid solution regions that allow the formation of heterojunctions is an important factor for the use of semiconductor compounds in electronics. Therefore, the existence of a large range of solid solutions with Ag₂Se (up to 60 mol % Ag₂Se) is important for the prospects of using Ag₂S in flexible electronics [5, 6]. Moreover, it is especially important that Ag₂S in the monolithic state has a band gap width of $\Delta E_g = 1$ eV, while that of Ag₂Se is about 0.1 eV [7, 8]. This allows us to change the value of ΔE_g in solid solutions over a wide range of values. Interest in silver chalcogenides is also due to the fact that an important parameter for electronics in general and flexible electronics in particular is the mobility of carriers. Its growth allows us not only to increase performance but also to increase the resolution of displays. Thus, an increase in carrier mobility in devices based on complex indium, gallium, and zinc oxide (IGZO) by 20–50 times compared to amorphous silicon traditionally used in flexible electronics allowed Sharp to release flexible displays with a resolution of 10^3 pixels per inch. The carrier mobility in IGZO increases rapidly with the increasing free carrier concentration (n) and tends to 15 cm²/Vs at $n = 10^{18}$–10^{19} cm⁻³ [9]. Electron carrier mobility in Ag₂Se at room temperature is

Table 1. Purity of the reagents used

Substance	Reagent grade	Purity, %	Possible impurities
Silver	Refined	99.99	Cu, Pt, Pd, Fe
Selenium	Extra pure 17-3	99.997	S, Al, Sn
Sulfur	Extra pure 16-4	99.9998	Se, Al, P

almost two orders of magnitude higher (1000 cm^2/V s [10, 11]).

Knowledge of the properties of silver chalcogenides is of particular importance for the development of chalcogenide glasses: semiconductor materials for IR optics. The introduction of the specified compounds in their composition allows us not only to increase the plasticity of glass [4] and relax mechanical stresses but also to maintain relatively high softening temperature values [12]. This combination of thermal and mechanical properties of glass significantly improves their performance characteristics.

MEASUREMENT TECHNIQUE

Silver chalcogenides were synthesized from elemental components: silver, sulfur, and selenium. The quality and grade of the starting components are given in Table 1.

The starting components were weighed on an analytical balance with an accuracy of $\pm 10^{-4}$ g and placed in sealed quartz ampules from which air was pumped out to a vacuum of 10^{-4} mm Hg. The synthesis was carried out in a muffle furnace at a temperature of 900°C with constant stirring for three hours. The ampules were cooled in air.

To obtain cylindrical samples, the resulting ingots were pressed under a pressure of 20 MPa. An example of the obtained sample is shown in Fig. 1a.

Foil samples (Fig. 1b) and wires (Fig. 1c) were obtained by cold rolling. The minimum foil thickness was 30 μm and was limited by the adjustment accuracy of the rolling device.

The Vickers microhardness measurement method involves pressing a regular tetrahedral diamond pyramid into a sample and measuring the diagonal of the resulting imprint. Vickers microhardness is determined by the following formula: $H_V = \dfrac{2P \sin \dfrac{\alpha}{2}}{d^2}$, where α is the angle between the opposite edges of the pyramid, d is the length of the diagonal of the print, and P is the load value. The load holding time of 100 g was 10 sec. The result was taken as the average value of microhardness for a series of 10 measurements.

The density (ρ) of the studied glass samples weighing 3–4 g was determined by hydrostatic weighing in toluene at a temperature of 25°C. The density of toluene was previously determined using the reference sample, which was single-crystal germanium. Each sample was weighed several times, and the density value was considered to be the average value based on the sum of all measurements. The accuracy of density determination is ± 0.001 g/cm^3.

The pulse-phase method was used to measure the speed of ultrasonic waves. The operating frequencies of the probing pulses were 4 MHz for measuring longitudinal wave velocities and 2.3 MHz for measuring transverse wave velocities. This choice of frequencies ensured consistency between sample sizes and wavelengths.

The samples for recording optical absorption spectra in the visible and infrared regions of the spectrum were foils obtained by cold rolling. In the region of short wavelengths (from 500 to 3000 nm), measurements were carried out on a Shimadzu UV-3600 device with a slit width of 5.0. In the long-wave region (3–25 μm), measurements were carried out on a Bruker Tensor 27 spectrophotometer.

XRD measurements were carried out on a D8 Discover diffractometer (Bruker, Germany) using monochromated parallel Cu$K\alpha_1$ beam radiation. The diffraction patterns were processed by the full-profile modeling method using Topas 5.0 software (Bruker). The microstructural characteristics were determined
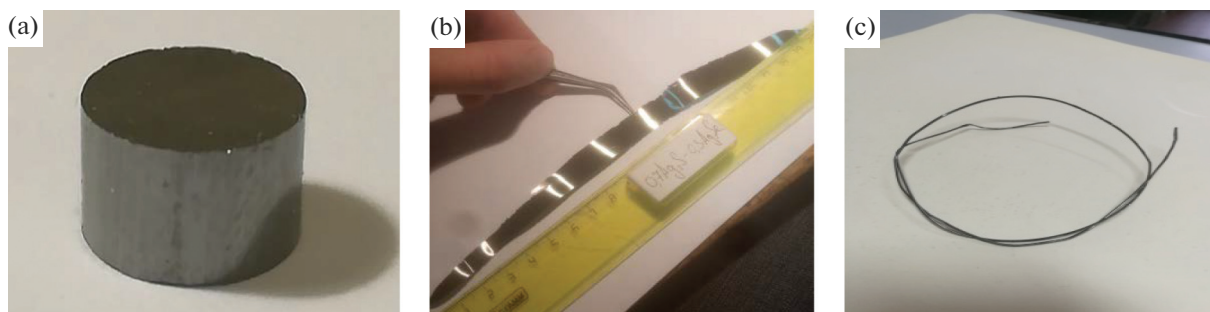

Fig. 1. Samples of solid solutions in the form of a cylinder obtained by pressing (a), as well as in the form of foil (b) and wire (c), obtained by cold rolling.

taking into account instrumental aberrations using standardization using the LaB_6 (NIST SRM 660a) standard sample, taken under similar conditions. Here, the crystallite size is understood as the volume-weighted average length of elementary columns (coherent length), averaged over all directions.

The Seebeck coefficient measurements on cylindrical samples with a diameter of 4.5 mm and a height of 3 to 4 mm were carried out on a PPMS (physical property measurement system produced by Quantum Design) setup using the thermal transport option. Heat was supplied to one end of the sample from a heating element, and the Seebeck effect was estimated as the ratio of the potential difference at the ends of the sample to the temperature difference. In addition, the Seebeck coefficient measurements were carried out on a rolled wire with a cross section of 1 mm and a length of 0.5 m. The temperature of one of the ends was maintained at 0°C; and of the other end, at 100°C A wire of chromel or alumel was connected to both ends, and the potential difference was measured using a conventional digital multimeter.

The study of the electrical conductivity of the samples was carried out using impedance spectroscopy in the frequency range of 1 MHz to 100 Hz. For this purpose, the Autolab PGSTAT302 potentiostat/galvanostat was used. The volumetric samples for measurements had a cylindrical shape: diameter 4.5 mm, height 3–4 mm, film sample are 8.5×6.5 mm^2, and 50–150 microns thick. To obtain Ag electrodes, Degussa brand silver paste was used. Impedance measurements were carried out in the temperature range of 20–150°C in a quartz glass cell in air. The temperature in the measuring cell was maintained by a microprocessor measuring instrument and controller TRM101 (OVEN) with an accuracy of ±0.1°C and was controlled by a digital voltmeter 34420A (Agilent) with a chromel-alumel thermocouple.

The resistance value of the samples was found by extrapolating the impedance spectrum to the active resistance axis using the ZView program (Scribner Associates, Inc (Version 3.3c)). Electrical conductivity was calculated using the formula $\sigma = \dfrac{l}{SR}$, where R is the resistance of the sample, l is its thickness, and S is the cross-sectional area.

RESULTS AND DISCUSSION

Polycrystalline alloys of the system $(1 - x)Ag_2S - xAg_2Se$ were obtained by high-temperature synthesis. For x ranging from 0 to 0.6, they form solid solutions with a monoclinic structure based on Ag_2S (solid solutions I). With x ranging from 0.7 to 1, they form solid solutions with an orthorhombic structure based on Ag_2Se (solid solutions II) [5, 6]. In order to study the mechanical properties of these alloys, the concentration dependencies of the propagation velocity of the

transverse (V_t) and longitudinal (V_l) ultrasonic waves, density (ρ), as well as Vickers microhardness (H_V), were studied (Fig. 2a). Based on these data, Poisson's ratio (ν), Young's modulus (E), and Grüneisen parameter (γ) were calculated (1–3) using the following equations. These parameters are given in Table 2. The plasticity (δ_H) calculated using Eq. (4) according to Milman [13] is shown in Fig. 2c.

$$\nu = \frac{2 - a}{2(1 - a)}, \quad a = \left(\frac{V_l}{V_t}\right)^2, \tag{1}$$

$$E = \frac{V_l^2 \rho (1 + \nu)(1 + 2\nu)}{1 - \nu} = 2V_t^2 \rho (1 + \nu), \tag{2}$$

$$\gamma = \frac{3}{2}\left(\frac{1 + \nu}{2 - 3\nu}\right), \tag{3}$$

$$\delta_H = 1 - 14.3\left(1 - \nu - 2\nu^2\right)\frac{H_V}{E}. \tag{4}$$

H_V of solid solutions I decreases with the introduction of Ag_2Se right up to $x = 0.6$. While the introduction of Ag_2S in Ag_2Se leads to a significant increase in microhardness (Fig. 2a). This gave grounds to believe that solid solutions of I with a monoclinic crystal lattice have an abnormally high plasticity, exceeding the plasticity of Ag_2S. Solid solutions II, however, apparently have lower plasticity. It is interesting to compare the obtained concentration dependence of microhardness with the concentration dependence of the enthalpy of mixing of solid solutions [5].

From Fig. 2a it is clear that, with an increase in the molar fraction of Ag_2Se in solid solutions $(1 - x)Ag_2S - xAg_2Se$ from $x = 0$ to 0.6, the absolute value of the mixing energy (interaction) of the components increases slightly [5]. The very fact of its increase is due to the fact that the ratio of the mixed components tends to 1. The same thing, but to a much greater extent, happens in the range from $x = 0.7$ to 1. From $x = 0.6$ to 0.7, the components of the system do not mix, and the mixing energy is zero. Due to the fact that the slope of the graph in the region of solid solutions II is much greater than in region I, it can be concluded that the solution based on Ag_2Se is characterized by a stronger interaction of its components (and, consequently, a greater degree of their ordering) than the solid solution based on Ag_2S. This leads to a decrease in the volume of the unit cell compared to the additive dependence (Fig. 2b), while in the region of solid solutions I, on the contrary, a certain increase in the volume of the unit cell is observed. This behavior of the mixing energy and the unit cell volume is closely correlated with the increase in microhardness upon the introduction of Ag_2S in Ag_2Se (solid solution region II, see Fig. 2a). At the same time, the introduction of Ag_2Se in Ag_2S leads to some decrease in microhardness. A natural result of such behavior of the listed properties is an increase in plasticity in the region of
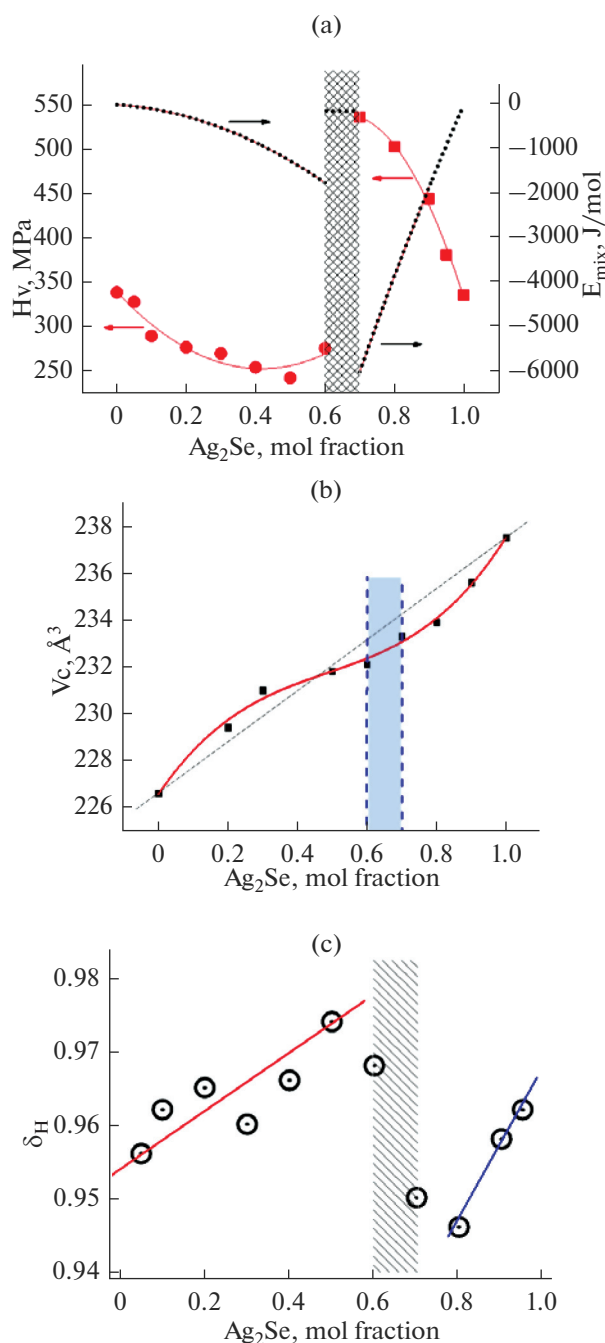
(a)

(b)

(c)

Fig. 2. (a) Red circles and squares are the concentration dependence of microhardness for two regions of solid solutions (our data). The dashed black lines are the mixing energy for solid solutions (I) and (II) at 298° K [5]. The shaded area separates the Ag$_2$S-based solid solutions and Ag$_2$Se-based solid solutions. (b) Concentration dependence of the unit cell volume for two regions of solid solutions [6]. (c) Concentration dependence of plasticity according to Milman (our data).

solid solutions I and its decrease in the region of solid solutions II (Fig. 2c). Therefore, solid solutions I can be subjected to all types of mechanical treatment, including cold rolling (Figs. 1b, 1c). Solid solutions II

are destroyed by attempts at cold rolling, but can be pressed and drilled.

The works [14−16] point out the direct relationship between Poisson's ratio and the plasticity of not only metals but also other materials. In particular, for metals, a significant increase in ductility is observed when Poisson's ratio is greater than 0.32. In relation to this, it should be noted that all Poisson's ratio values given in Table 2 exceed this value. The maximum value of this parameter is 0.43, which is close to the value of Poisson's ratio for absolutely incompressible materials, such as water ($\nu = 0.5$).

The studied materials are of interest not only due to their high plasticity. In addition, they are semiconductors. Moreover, as noted in the introduction, the values of the band gap width for the extreme components of the studied system differ by an order of magnitude. In combination with the existence of an extended region of solid solutions I, this gives us grounds to hope that heterojunctions can be obtained. This explains the interest in studying the semiconductor properties of these materials.

The optical absorption spectra were studied in the near, middle, and far IR spectral regions on foil samples obtained by cold rolling (Fig. 3). Their thickness did not exceed 150 microns. This made it possible to achieve high optical absorption coefficients and correctly determine the fundamental absorption edge according to Tauc. The concentration dependence of the optical band gap for direct interband transitions determined in this way actually demonstrates a significant change from 0.9 eV for pure Ag$_2$S up to 0.45 eV for an equimolar solid solution (Fig. 3).

The optical absorption spectrum shows a wide transparency region up to at least 25 μm. The results of the Raman scattering study of silver chalcogenides do not reveal Raman bands in the high-frequency region up to 200 cm^{-1} [17]. Therefore, it cannot be ruled out that the transparency region extends up to 50 μm. In the wavelength range from the fundamental absorption edge to 10 μm, a scattering tail on crystalline grains is observed. This is consistent with the results of X-ray diffraction studies (Table 3), which indicate that the most probable size of crystalline grains is 100 nm.

Figure 4a shows the concentration dependence of the Seebeck parameter of the solid solutions studied. The negative sign indicates electronic conductivity. The absolute value of the Seebeck coefficient, as expected, increases with the increasing band gap. The asterisk in the figure indicates the value of the Seebeck coefficient for an equimolar solid solution, obtained by the classical method. In other words, several meters of semiconductor wire were obtained by cold rolling. This wire was then used to make classical thermocouples in combination with wires of various metals for which the Seebeck coefficient values were known. The measured thermoelectric power of the manufactured

Table 2. Properties of alloys in the $(1 - x)Ag_2S-xAg_2Se$ system (Compositions belonging to the field of solid solutions based on Ag_2S are highlighted in bold)

x	V_l, m/sec	V_s, m/sec	Density (ρ), g/cm³	Poisson coefficient (ν)	Young's modulus (E), GPa	Grüneisen parameter (γ)
0.95	3200	1230	8.20	0.41	35.2	2.8
0.9	3320	1310	8.10	0.41	39.1	2.7
0.8	3140	1270	8.10	0.40	36.4	2.7
0.7	3350	1240	7.92	0.42	34.7	2.9
0.6	3010	1090	7.86	0.42	26.8	2.9
0.5	3140	1100	7.77	0.43	26.7	3.0
0.4	2860	1080	7.70	0.42	25.4	2.8
0.3	2780	1090	7.50	0.41	25.3	2.7
0.2	2950	1140	7.60	0.41	28.0	2.8
0.1	2930	1150	7.50	0.41	28.2	2.7
0.05	2930	1120	7.25	0.42	25.6	2.8

thermocouples made it possible to determine the value of the Seebeck coefficient of the semiconductor wire.

The results presented in Fig. 4b are particularly interesting. It compares the temperature dependencies of the specific electrical conductivity of the original solid solution of the ingots and foil obtained from them by cold rolling.

It is noteworthy that cold rolling did not lead to a change in either the activation energy of electrical conductivity or its absolute value. This means that even such a severe deformation does not lead to the formation of electrically active defects in the crystal lattice. It is also possible that such defects arise directly

during the deformation process, but relax fairly quickly at room temperature.

The absence of significant changes in the crystal structure during mechanical deformation is also indicated by the results of the X-ray diffraction study (Table 3, Fig. 5). One can speak of a tendency toward a decrease of the size of coherent X-ray scattering regions and increase in the degree of crystallinity as a result of mechanical processing. This change in morphology is expected. There are no significant changes in the microstresses of the crystal lattice. It is noteworthy that the degree of crystallinity of the samples is different from 1. Apparently, both silver sulfide and sele-
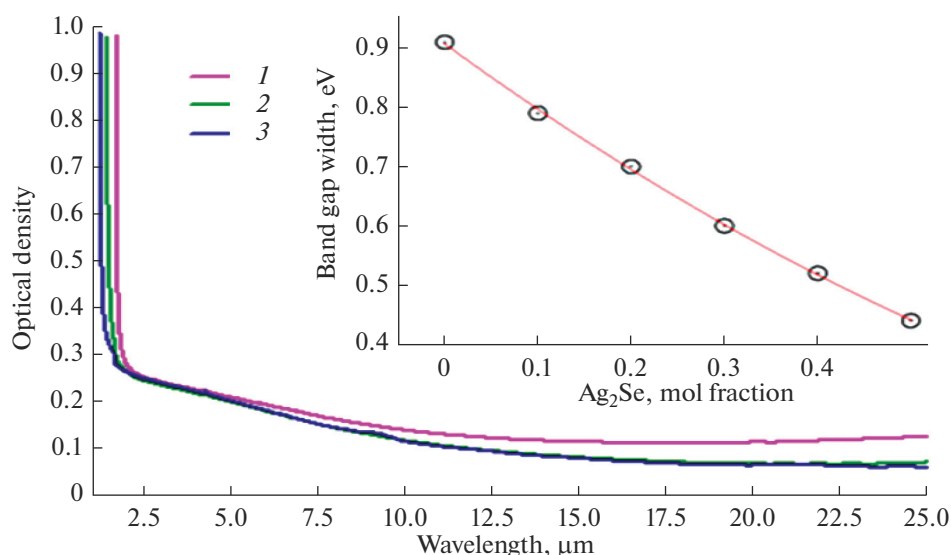

Fig. 3. Survey spectrum of optical absorption in the IR range. (*1*) 0.2 Ag_2Se, (*2*) 0.1 Ag_2Se, (*3*) 0 Ag_2Se. The inset shows the concentration dependence of the optical band gap.

Table 3. Comparison of crystal lattice parameters for monolithic ingots and for foil obtained from them by cold rolling according to X-ray diffraction data

Composition	Ag$_2$(S$_{0.8}$Se$_{0.2}$)		Ag$_2$S	
Parameter	ingot	roll	ingot	roll
Degree of crystallinity, %	86	89	86	93
Crystal grain size, nm	120(70)	70(20)	160(80)	98(10)
Voltages, relative units	$8(2) \times 10^{-4}$	$7(2) \times 10^{-4}$	$5.3(1) \times 10^{-4}$	$6.4(1) \times 10^{-4}$
Unit cell parameters				
a, Å	4.2382(7)	4.2330(6)	4.2261(2)	4.2330(5)
b, Å	6.9374(8)	6.9456(9)	6.9278(4)	6.9107(6)
c, Å	8.3332(10)	8.3229(9)	8.2831(4)	8.2905(7)
beta, °	110.340(4)	110.279(5)	110.563(3)	110.699(5)
Volume of the unit cell, Å^3	229.74(5)	229.53(5)	227.06(2)	226.87(4)
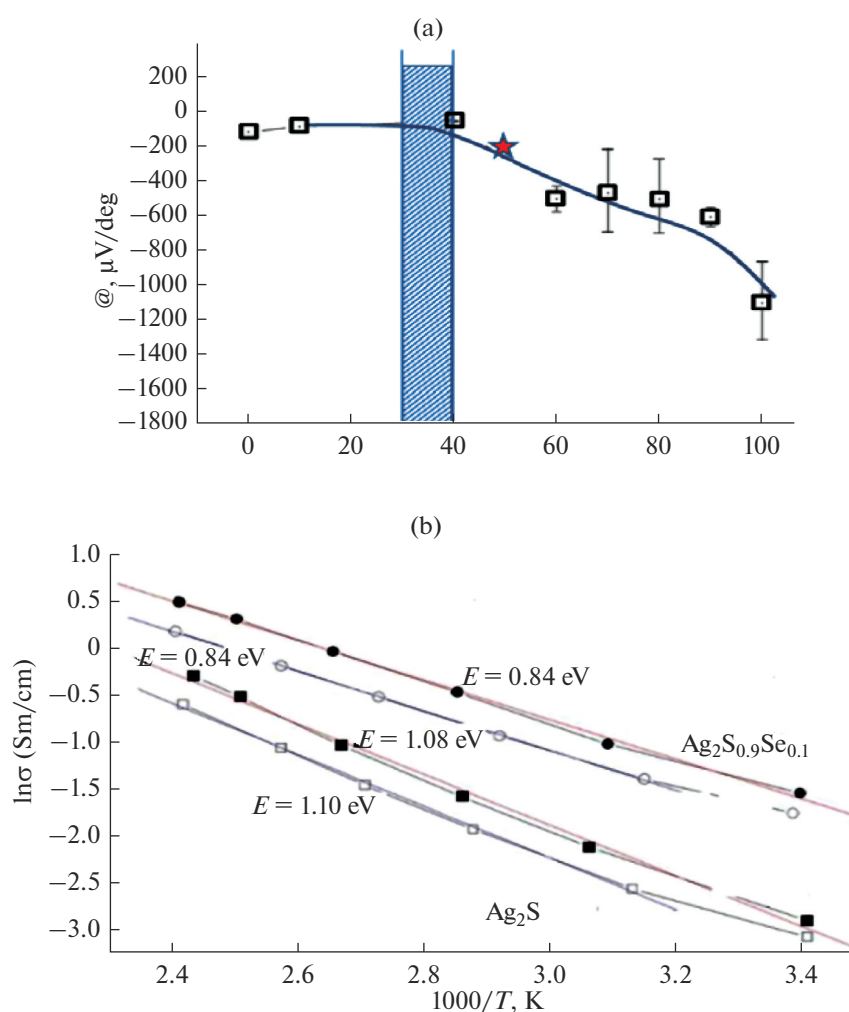
Fig. 4. (a) Concentration dependence of the Seebeck constant. The asterisk marks the result obtained by measuring the thermoelectric power of thermocouples twisted from the wire of the studied semiconductor and the wires of reference metals. (b) Temperature dependencies of the specific conductivity of bulk samples (light squares and circles) and film samples obtained from them by rolling (dark circles and squares). The composition of the samples and the activation energies of conductivity are shown in the figure.
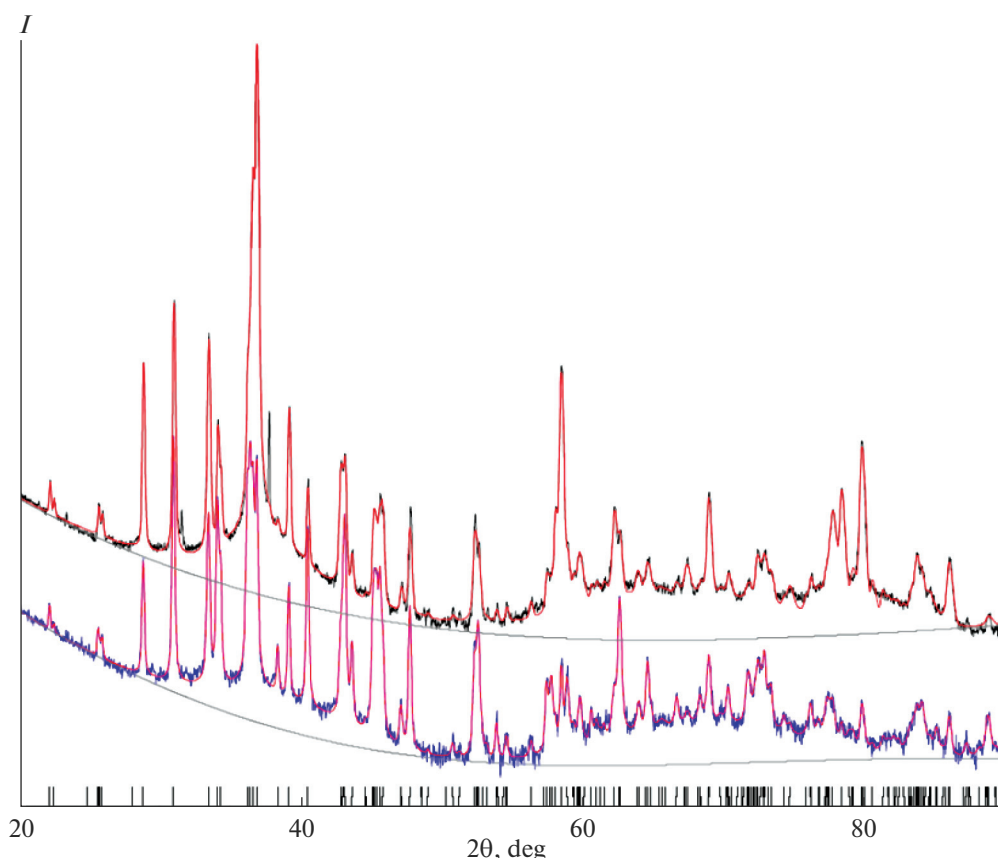
Fig. 5. Comparison of diffraction patterns of the original Ag$_2$S ingot (lower) and foil obtained from it by cold rolling (upper).

nide, due to metallophilic interactions, have some tendency toward glass formation. In relation to this, it should be noted that the authors [18] observed highly dispersed liquation regions in glasses of the $(Ge_xSe_{1-x})_{1-y}$–Ag_y system, whose chemical composition coincided with the Ag$_2$Se compound. In [19, 20] stoichiometric Ag$_2$Se films, which were amorphous in their original state, were obtained by laser deposition. Their amorphous state is stable, and crystallization requires heating to a temperature of at least 150°C and subsequent cooling.

FUNDING

CONFLICT OF INTEREST

The authors of this work declare that they have no conflicts of interest.

REFERENCES

1. Shi, X., Chen, H., Hao, F., Liu, R., Wang, T., Qiu, P., Burkhardt, U., Grin, Yu., and Chen, L., Room-temperature ductile inorganic semiconductor, *Nat. Mater.*, 2018, vol. 17, no. 5, pp. 421–426.
https://doi.org/10.1038/s41563-018-0047-z

2. Tveryanovich, Yu.S., Fazletdinov, T.R., Tverjanovich, A.S., Fadin, Yu.A., and Nikolskii, A.B., Features of chemical interactions in silver chalcogenides responsible for their high plasticity, *Russ. J. Gen. Chem.*, 2020, vol. 90, no. 11, pp. 2203–2204.
https://doi.org/10.1134/s1070363220110304

3. Evarestov, R.A., Panin, A.I., and Tverjanovich, Yu.S., Argentophillic interactions in argentum chalcogenides: First principles calculations and topological analysis of electron density, *J. Comput. Chem.*, 2021, vol. 42, no. 4, pp. 242–247.
https://doi.org/10.1002/jcc.26451

4. Tveryanovich, Yu.S., Fazletdinov, T.R., Tverjanovich, A.S., Pankin, D.V., Smirnov, E.V., Tolochko, O.V., Panov, M.S., Churbanov, M.F., Skripachev, I.V., and Shevelko, M.M., Increasing the plasticity of chalcogenide glasses in the system Ag$_2$Se–Sb$_2$Se$_3$–GeSe$_2$, *Chem. Mater.*, 2022, vol. 34, no. 6, pp. 2743–2751.
https://doi.org/10.1021/acs.chemmater.1c04312

5. Pal'yanova, G.A., Chudnenko, K.V., and Zhuravkova, T.V., Thermodynamic properties of solid solutions in the system Ag$_2$S–Ag$_2$Se, *Thermochim. Acta*, 2014,

vol. 575, pp. 90−96.
https://doi.org/10.1016/j.tca.2013.10.018

6. Pingitore, N.E., Ponce, B.F., Eastman, M.P., Moreno, F., and Podpora, C., Solid solutions in the system Ag$_2$S−Ag$_2$Se, *J. Mater. Res.*, 1992, vol. 7, no. 8, pp. 2219−2224.
https://doi.org/10.1557/jmr.1992.2219

7. Dalven, R. and Gill, R., Energy gap in ?−Ag$_2$Se, *Phys. Rev.*, 1967, vol. 159, no. 3, pp. 645−649.
https://doi.org/10.1103/PhysRev.159.645

8. Zhao, Zh., Wei, H., and Mao, W.L., Pressure tuning the lattice and optical response of silver sulfide, *Appl. Phys. Lett.*, 2016, vol. 108, no. 26, p. 261902.
https://doi.org/10.1063/1.4954801

9. Kimura, M., Kamiya, T., Nakanishi, T., Nomura, K., and Hosono, H., Intrinsic carrier mobility in amorphous In−Ga−Zn−O thin-film transistors determined by combined field-effect technique, *Appl. Phys. Lett.*, 2010, vol. 96, no. 26, p. 262105.
https://doi.org/10.1063/1.3455072

10. Somogyi, K., Panine, P., and Sáfrán, G., Temperature dependence of the carrier mobility in Ag$_2$Se layers grown on NaCl and SiO$_x$ substrates, *Acta Phys. Hung.*, 1994, vol. 74, no. 3, pp. 243−255.
https://doi.org/10.1007/bf03156304

11. Mi, W., Qiu, P., Zhang, T., Lv, Ya., Shi, X., and Chen, L., Thermoelectric transport of Se-rich Ag$_2$Se in normal phases and phase transitions, *Appl. Phys. Lett.*, 2014, vol. 104, no. 13, p. 133903.
https://doi.org/10.1063/1.4870509

12. Tver'yanovich, Yu.S., Fazletdinov, T.R., and Tomaev, V.V., Peculiarities of the effect of silver chalcogenides on the glass-formation temperature of chalcogenide glasses with ionic conduction, *Russ. J. Electrochem.*, 2023, vol. 59, no. 8, pp. 567−572.
https://doi.org/10.1134/s1023193523080086

13. Milman, Yu.V., Chugunova, S.I., Goncharova, I.V., and Golubenko, A.A., Plasticity of materials determined by the indentation method, *Usp. Fiz. Met.*, 2018, vol. 19, no. 3, pp. 271−308.
https://doi.org/10.15407/ufm.19.03.271

14. Gu, X.J., Mcdermott, A.G., Poon, S.J., and Shiflet, G.J., Critical Poisson's ratio for plasticity in Fe−Mo−C−B−Ln bulk amorphous steel, *Appl. Phys. Lett.*, 2006, vol. 88, no. 21, p. 211905.
https://doi.org/10.1063/1.2206149

15. Yang, G.N., Sun, B.A., Chen, S.Q., Gu, J.L., Shao, Y., Wang, H., and Yao, K.F., Understanding the effects of Poisson's ratio on the shear band behavior and plasticity of metallic glasses, *J. Mater. Sci.*, 2017, vol. 52, no. 11, pp. 6789−6799.
https://doi.org/10.1007/s10853-017-0917-9

16. Sanditov, D.S., Mantatov, V.V., and Sanditov, B.D., Poisson ratio and plasticity of glasses, *Tech. Phys.*, 2009, vol. 54, no. 4, pp. 594−596.
https://doi.org/10.1134/s1063784209040240

17. Ge, J.-P. and Li, Y.-D., Ultrasonic synthesis of nanocrystals of metal selenides and tellurides, *J. Mater. Chem.*, 2003, vol. 13, no. 4, pp. 911−915.
https://doi.org/10.1039/b210077k

18. Mitkova, M., Wang, Yu., and Boolchand, P., Dual chemical role of Ag as an additive in chalcogenide glasses, *Phys. Rev. Lett.*, 1999, vol. 83, no. 19, pp. 3848−3851.
https://doi.org/10.1103/physrevlett.83.3848

19. Tveryanovich, Yu.S., Razumtcev, A.A., Fazletdinov, T.R., Tverjanovich, A.S., and Borisov, E.N., Fabrication of stoichiometric oriented Ag$_2$Se thin film by laser ablation, *Thin Solid Films*, 2018, vol. 666, pp. 172−176.
https://doi.org/10.1016/j.tsf.2018.09.036

20. Tveryanovich, Yu.S., Razumtcev, A.A., Fazletdinov, T.R., Krzhizhanovskaya, M.G., and Borisov, E.N., Stabilization of high-temperature Ag$_2$Se phase at room temperature during the crystallization of an amorphous film, *Thin Solid Films*, 2020, vol. 709, p. 138187.
https://doi.org/10.1016/j.tsf.2020.138187

SPELL: 1. OK